Parametric analysis of ground source heat pump system for heating of office buildings in Nordic climate

Conference Paper · October 2020

CITATIONS
0

READS
40

4 authors:

Mehrdad Rabani
Oslo Metropolitan University
21 PUBLICATIONS **95** CITATIONS
SEE PROFILE

Habtamu B. Madessa
Oslo Metropolitan University
16 PUBLICATIONS **84** CITATIONS
SEE PROFILE

Jørgen Torgersen
Oslo Metropolitan University
1 PUBLICATION **0** CITATIONS
SEE PROFILE

Natasa Nord
Norwegian University of Science and Technology
84 PUBLICATIONS **805** CITATIONS
SEE PROFILE

Parametric analysis of ground source heat pump system for heating of office buildings in Nordic climate

Mehrdad Rabani[1,2*], Habtamu Bayera Madessa[1], Jørgen Torgersen[3], Natasa Nord[2]
[1]Department of Civil Engineering and Energy Technology, Oslo Metropolitan University, Oslo, Norway
[2]Department of Energy and Process Engineering, Norwegian University of Science and Technology, Trondheim, Norway
[3]Asplan Viak AS, Norway
* *Mehrdad Rabani: Mehrdad.Rabani@oslomet.no*

Abstract

This paper presents a sensitivity analysis followed by an optimization to improve the performance of a ground source heat pump (GSHP) system for an office building located in Norway, for Oslo, Stavanger, and Tromsø climatic conditions. The ground source heating model was firstly validated by available measured data. The sensitivity and optimization simulations were conducted by using IDA ICE software and its integration with the GenOpt tool for optimization. The sensitivity results showed that the borehole depth was the most prominent parameter. Therefore, by increasing and decreasing the borehole length by 20%, for example for Tromsø climatic condition, the energy supplied by the top heating reduced by 22% and increased by 31%, respectively.

Introduction

Buildings contribute around 33% to the greenhouse gas emissions. Therefore, reducing the energy use of the building stock may significantly decrease the global CO_2 emissions (Metz et al., Ally et al.). To have a substantial impact, a deep retrofitting is essential. Therefore, in addition to improvements of the building envelope, utilization of renewable energy sources in the energy supply system of buildings should increase. Ground energy source is an example in this point, which is a clean and available renewable energy that has shown a great potential for heating applications, especially in cold climate countries such as Norway (Nord et al. 2016, Nord 2017). Many researchers have investigated different ways to reduce the building energy use by taking advantage of ground energy source.

A ground source heat pump (GSHP) is an efficient method for extracting energy from the ground and use for heating applications. As the earth has a relatively constant temperature at depth, this technology can transfer the stored heat in ground to the building site. Several studies analyzed this system. Madessa et al. conducted a parametric study to assess the performance of the GSHP with vertical bore holes configuration. The results showed that ground depth is an important factor affecting the coefficient of performance (COP) of the GSHP significantly. Further, Wang et al. analyzed the potential of the GSHP by modelling the energy use of a conventional building under various climatic conditions. They found out that the thermal conductivity of local geological materials could considerably affect the system performance. Integration of the GSHP with other technologies such as solar thermal collectors (Emmi et al., Naranjo-Mendoza et al.), concentrated photovoltaic thermal solar collectors (Chen et al.), and heat recovery and exhaust air heat pump (Nord et al., Zhang et al.) proved to be a robust solution for heating application in cold climate countries.

This study performed a sensitive and optimization analyses on different parameters of a the GSHP system in cold climatic condition in order to identify the influential system parameters and find their best combination set that could result in minimum delivered energy to the building for space heating application.

Theoretical Background

A compression based heat pump is a machine used to transfer heat from a low temperature source to a high temperature sink (application area) by using the compression work. It consists mainly of an evaporator, a compressor, a condenser, and an expansion valve. The heating performance of the heat pump is evaluated using a factor called coefficient of performance (COP) indicating the ratio between the useful heat supplied by the heat pump condenser and the required work input to the compressor.

In a GSHP, a secondary loop system transfers the heat from the heat pump to the building. The ground borehole, which transfers the heat from the circulating fluid to the heat pump loop, could be buried horizontally or vertically. The amount of thermal energy extracted from the ground depends on borehole depth, number of boreholes, and radius of boreholes, mass flow rate of the working fluid as well as the conductivity of ground and filling mass of borehole.

Method

To study the effect of different parameters on the performance efficiency of the GSHP system, IDA-ICE energy simulation software was used. Furthermore, to

optimize the system input parameters for improving the GSHP performance, IDA-ICE was coupled with the GenOpt optimization tool.

Borehole modeling for validation

To validate the borehole extension model in IDA-ICE, numerical results were validated by the available measured data taken from the Powerhouse Kjørbo's ground heating system, located in Bærum, Norway. It should be noted that the borehole extension model in IDA-ICE was also validated by Fadejev and Kurnitski.

The results for the temperature of the brine liquid at the outlet of the borehole and the thermal performance of the soil were compared. This was done by controlling the type of brine liquid, its mass flow rate and pressure, and the brine liquid temperature at the inlet of the borehole. Figure 1 shows the location, configuration, and schematic of the vertical boreholes considered for the validation study.

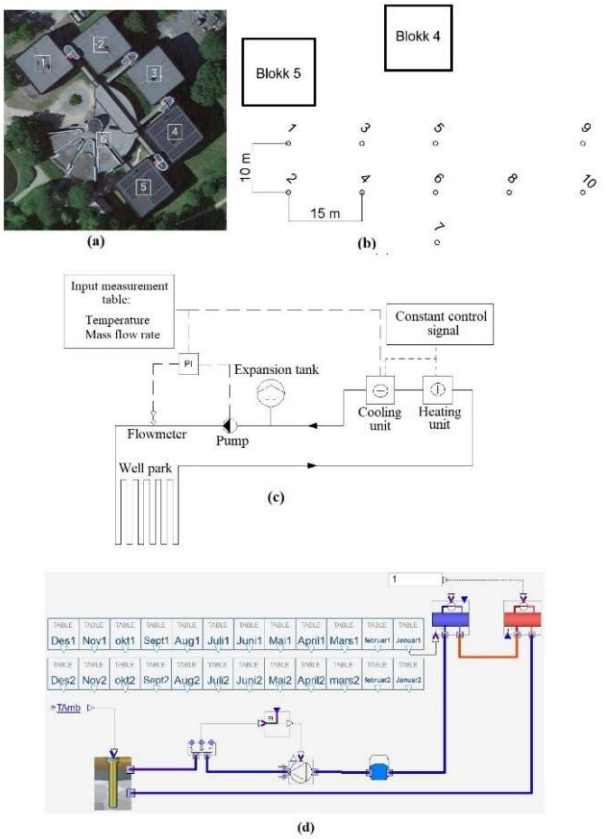

Figure 1. (a) Location and (b) configuration of boreholes, (c) schematic, and (d) simulated model of vertical borehole system

In the simulation model for the borehole system for validation, the heat carrier, from the outlet of the well park, flowed through a heating unit and then passed through a cooling unit and reached the real measured temperature. The real measured temperature was the brine liquid temperature at the inlet of the borehole, was given as an input table in Figure 1 (c). The cooling and heating units had a constant control signal equal to 1, meaning that they are switched on all the time and they can adjust the brine liquid temperature at the inlet of the borehole to those of measurements. The circulation pump received a control signal from a PI controller to keep the measured mass flow at the set point value. It is worth mentioning that the table values in the simulation (Figure 1 (d)) were averages of all the collected logged values from Kjørbo. The logged values from Kjørbo was collected every other minute.

The borehole temperatures in IDA ICE were modelled by ten nodes, evenly distributed over the borehole length. In addition, the borehole had input value for the outdoor air temperature to calculate the temperature in the ground and at the surface. In the borehole model, the average temperature in the soil as well as a temperature gradient should be stated. These were implemented as explained in Table 1. In addition, other information about the parameters used for validation of borehole model, including borehole properties, are listed in this table

Sensitive analysis and optimization settings

Figure 2(a) shows the floor plan and shape of the reference office building considered for sensitive analysis and optimization study. The office building met the requirements for Norwegian passive house standard according to the NS 3701 standard and had a heated area of 4 903 m^2. Energy calculations for the building were carried out in accordance with the NS 3031 Norwegian standard as described in the Norwegian building code TEK17.

Table 1. Detail of parameter values used for validation of borehole model

Parameter	Value
Borehole depth (m)	219
Borehole radius (m)	0.0575
Borehole casing (m)	6
Number of boreholes	10
Number of collector tubes per borehole	1
Collector pipe radius	0.016
Thickness of the collector tube (m)	0.024
Surface heat capacity (J/(kg·K))	1140
Surface conductivity (W/(m·K))	0.75
Surface density (kg/m^3)	1680
Ground heat capacity (J/(kg·K))	920
Ground conductivity (W/(m·K))	2.25
Ground density (kg/m^3)	2880
Temperature in ground (°C)	$\theta_m + 2$
Geothermal temperature gradient (°C/m)	0.02
Heat capacity of collector tube (J/(kg·K))	930
Conductivity of collector tube (W/(m·K))	0.41
Roughness of collector tube	1.524×10^{-4}
Heat capacity of filling mass (J/(kg·K))	420
Conductivity of filling mass (W/(m·K))	0.6
Density of filling mass (Kg/m^3)	1000

Type of brine liquid	Ethanol
Freezing temperature of brine liquid (°C)	-17
Conductivity of heat carrier	0.41

θ_m: Annual average air temperature (°C)

After the validation of the borehole extension model in IDA-ICE for Oslo climate, the model was tested for a generic office building for three different climatic conditions; Oslo, Stavanger, and Tromsø. The reference building energy supply system for the sensitive and optimization analysis was implemented using the Early Stage Building Optimization (ESBO) plant in IDA ICE (Figure 2(b)). It included peak load heating, base load heating, and heating and cooling distribution systems. The domestic hot water set point temperature was set to 55°C and the supply temperature to the hot water accumulation tank had was controlled by the outdoor compensation curve. To control the temperatures, a 3K dead-band was also considered for ventilation and space heating systems to avoid a high frequency from the actuators. The cold water temperature set points for ventilation air and space cooling units were 5°C and 14°C, respectively. Furthermore, the peak load heating was added to ensure that the heating set point temperatures were maintained in the upper part of accumulation tank all the time. To improve the GSHP efficiency and to avoid a low COP of the heat pump due to oversizing, the sizing of the entire plant was performed as the following: 80% of energy need for heating was covered by the base load heating from the GSHP condenser and the rest (20%) was covered by the peak load heating.

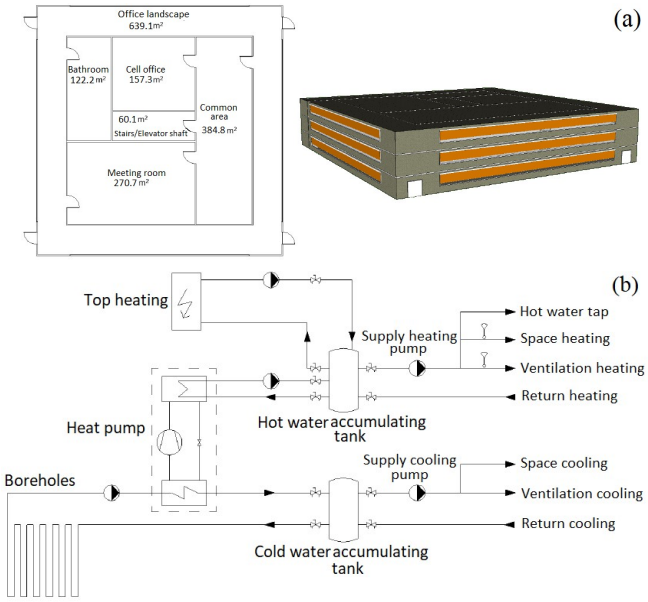

Figure 2. (a) Floor plan and shape of the office building and (b) the simplified schematic of energy supply system for sensitive and optimization study

The details of the building envelope and heating, ventilation, and air conditioning (HVAC) system are shown in Table 2. A hydronic heating system with radiators and convectors was used for space heating and cooling, respectively. The zone temperature set points for heating and cooling were 22 and 24°C, respectively.

Table 2. Details of building envelope, heat gains and HVAC system parameters in the reference case

Parameter	Value	Comment
Supply air temperature (°C)	16	Constant air volume (CAV) system
Supply air supply outside working hours (L/(s·m²))	0.7	Directorate of the Labor Inspectorate, profile usage: weekends, holidays, and non-working hours
Supply airflow during working hours (L/(s·m²))	2.1	Directorate of the Labor Inspectorate, profile usage: from 6:00 to 18:00 o'clock
Heat gain due to equipment (W/m²)	6	NS 3701, profile usage: from 7:00 to 18:00 o'clock, no usage in other times, holidays, and weekends
Heat gain due to occupancy (W/m²)	4	NS 3701, the same as equipment
Heat gain due to lighting (kWh/m²·year)	12.5	NS 3701, the same as equipment
U-Value (external wall/ceiling/floor) (W/(m²·K))	0.1/0.08 /0.08	NS 3701
U-Value (door/window) (W/(m²·K))	0.8/0.8	NS 3701
Normalized cold bridge	0.03	NS 3701
Efficiency of ventilation heat recovery	0.83	NS 3701
Specific fan power (kWh/(m³/s))	1	NS 3701
airtightness, n50 (h^{-1})	0.6	NS 3701

For sensitivity analysis, six parameters were considered and varied with ± 20% compared to the reference case, as shown in Table 3.

Table 3. Parameter values and ranges for sensitive analysis

Parameter	-20	Reference system	+20
Borehole depth (ZHOLE) (m)	175	219	263
Number of boreholes (NHOLE)	8	10	12
Conductivity of filling mass (K1) (W/(m·K))	0.48	0.6	0.72
Conductivity of ground (K2) (W/(m·K))	1.8	2.25	2.7
Mass flow rate (MFLOW) (kg/s)	1.6	2	2.4
Boreholes radius (RHOLE) (m)	0.046	0.0575	0.069

The optimization process was performed by using GenOpt tool with the combination of Particle Swarm

Optimization PSO and Generalized Pattern Search (GPS) with Hooke-Jeeves algorithms. The parameters considered for the optimization study are shown in Table 4. In the optimization process, the objective function was the delivered energy to the building.

Table 4. Range of parameter values considered for the optimization study

Parameter	Range	Description
Borehole depth (m)	50-400	Interval: 50
Number of boreholes	1-20	Interval: 1
Mass flow rate (kg/s)	1-5	Interval: 1
Tank radius (m)	0.1-1	Interval: 0.1
Window U-value ($W/(m^2.K)$)	0.6, 0.7, 0.8	NA

Results and discussion

Figure 3 shows the variation of the ground temperature in the reference borehole, simulated for ten evenly vertical points at three different cities.

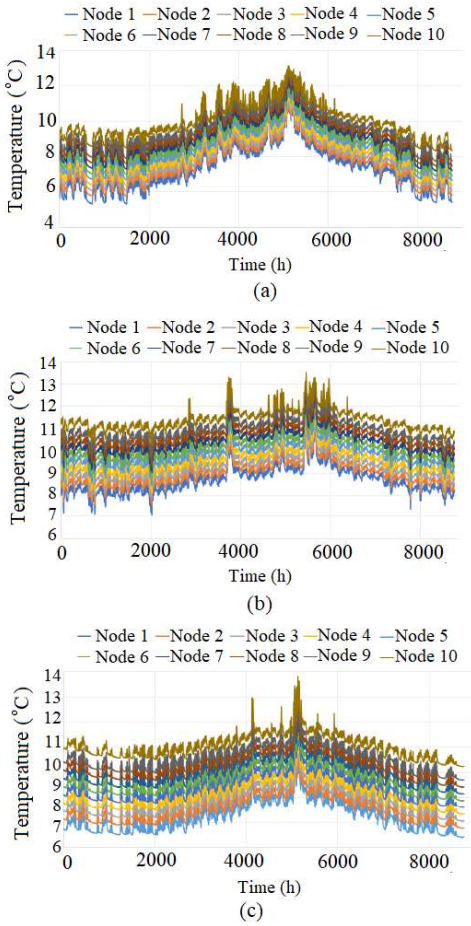

Figure 3. Annual ground temperature variation in the reference system at (a) Oslo, (b) Stavanger, and (c) Tromsø

A significantly higher ground temperature is observed for Stavanger compared to Tromsø and Oslo. The ground temperature was lower in winter and higher in summer due to transfer of heat from/to the ground to/from the building. It should be noted that the temperatures reached to their original level by the end of the year implying that a significant cooling of the ground did not cause over-discharging of ground on the annual level. However, this may be an issue over longer periods.

With regard to the parameters considered in Table 1, the numerical model of the boreholes was validated by the available measured data for Oslo climate, as shown in Figure 4(a) for the boreholes working fluid (ethanol) temperature at the outlet of boreholes and in Figure 4(b) the heat rate of chargning and discharing in the boreholes. The positive values mean extracting heat from the ground (discharging) and the negative values mean feeding heat to the ground (charging). It should be noted that Figure 4(b) shows the total charging and discharging in the boreholes. The maximum extraction rate from the ground was achieved around 18.3 $W/m_{borehole\ depth}$.

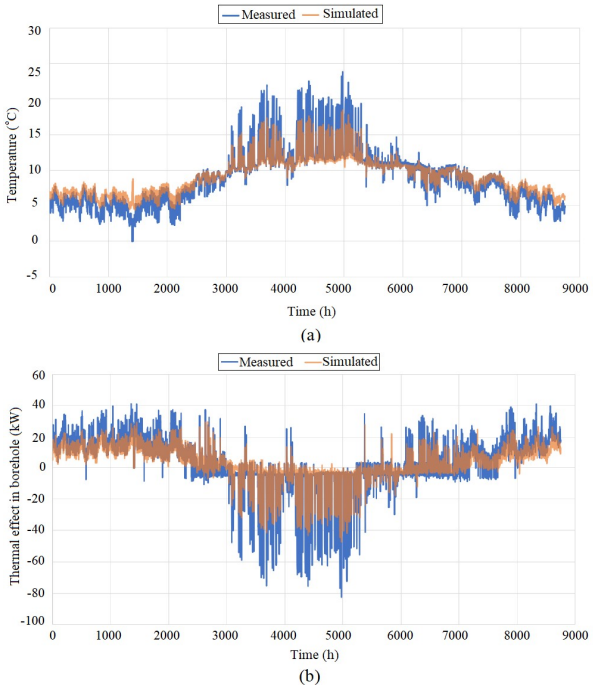

Figure 4. (a) Annual temperature variation of the brine liquid at the outlet of borehole and (b) Annual variation of charging and discharging in the boreholes

As it can be seen from Figure 4, the simulated results were in agreement with the measured data indicating the acceptable performance of the borehole extension model in IDA ICE in replicating the measured data. However, the measured values were higher than the simulated results and the average deviation between the measured and simulated results, e.g. for the brine liquid temperature at the outlet of borehole, was around 0.95 K.

Figure 5 compares the measured and the simulated values of the borehole working fluid temperatures at the outlet of the borehole. The comparison was also quantified using the Coefficient of Determination (R^2) and Coefficient of Variation of Root Mean Square Error (CV_{RMSE}) (ASHRAE), which the latter was defined as follows:

$$CV_{RMSE}(\%) = \frac{1}{\bar{y}}\sqrt{\frac{\sum_{i=1}^{n}(y_i - \hat{y}_i)^2}{n}} \times 100 \qquad (1)$$

where y_i is the simulated value at instance i, $\hat{y}_i$ is the measured value at instance i, $\bar{y}$ is the average of measured data, and n is the number intervals.

As Figure 5 shows R^2 is 96% implying that the variation in simulated temperature well followed the variation in measured temperatures. The CV_{RMSE} was also low, equal to 7% (should be less than 30% according to ASHRAE guideline), which indicated that measured values were in good agreement with the simulated values. It should be noted that the large discrepancies observed in Figure 4 were probably due to hourly averaging of the whole measured data set, shown in Figure 5.

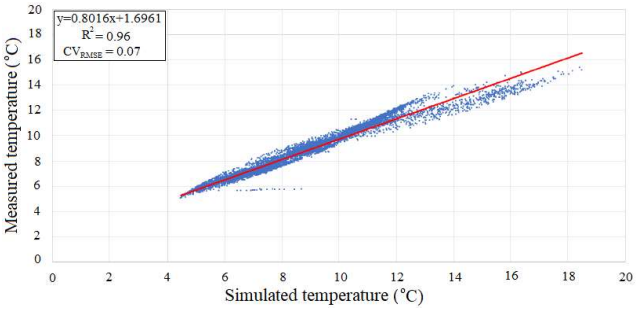

Figure 5. Scatter plot of measured and simulated annual temperature of working fluid at the outlet of borehole

After the borehole model was validated for the Oslo conditions, the model was tested for different climate conditions.

Figure 6 shows a qualitative spatial temperature variation in the ground for Tromsø when the ground temperature was 0°C simulated in IDA-ICE. The number of boreholes in this case was 10. Ground temperature variation reduced as the depth increased so that in far distance from the surface, the temperature remained almost constant and no further temperature variation with depth increase was observed.

The sensitivity analysis based on the parameters shown in Table 3 are presented here. Figure 7 shows the effect of 20% changes in the input parameters, as suggested in Table 3, on the compressor energy use, energy absorbed from the borehole, and the energy supplied by the peak load heating. The borehole depth was the most effective parameter on the borehole performance so that decreasing the borehole depth by 20% led the energy supplied by the peak load heating to increase up to 28%, 108%, and 31% for Oslo, Stavanger, and Tromsø climatic conditions, respectively. The corresponding increase of the borehole depth resulted the energy supplied by the peak load heating to decrease by 21%, 53%, and 22% respectively. Furthermore, the change in borehole parameters did not affect the energy extracted from the borehole and the compressor energy use as much as the heat supplied by the peak load heating for Stavanger. It is worth mentioning that the change in the borehole filling mass conductivity was not included in the results in Figure 7, because it had negligible effect on the energy use by the compressor, the extracted energy from the borehole, and the heat supplied by the peak load heating.

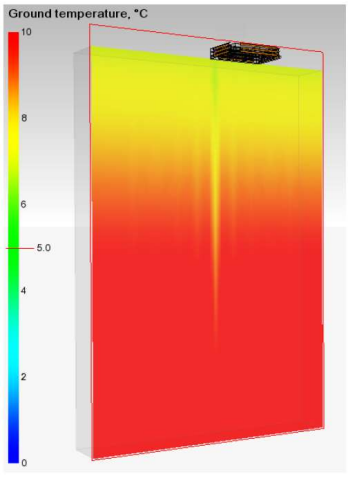

Figure 6. A cross section of temperature variation in the ground around the boreholes on 4th January for Tromsø climate

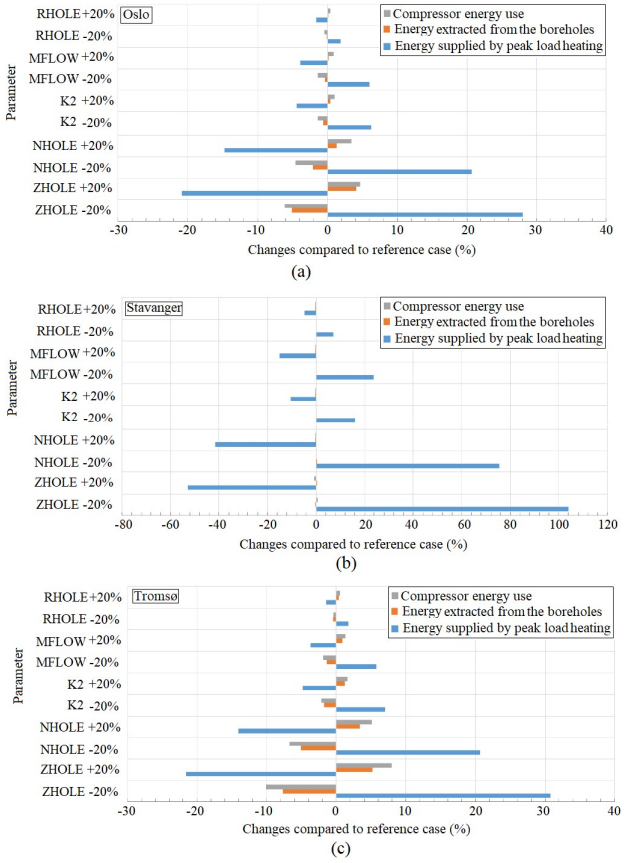

Figure 7. Tornado diagram of different parameters in sensitivity analysis for (a) Oslo, (b) Stavanger, and (c) Tromsø climatic conditions.

Figure 8 shows the impact of different parameters on the COP values at different cities. As it was also observed in Figure 7, the borehole length was the most influential factor on the COP. The COP values at Stavanger did not follow the same trend as in Tromsø and Oslo. The reason was the ratio between the amount of energy used by the compressor and the extraction energy from the borehole. This can be better explained, for example for borehole length, in Figure 9.

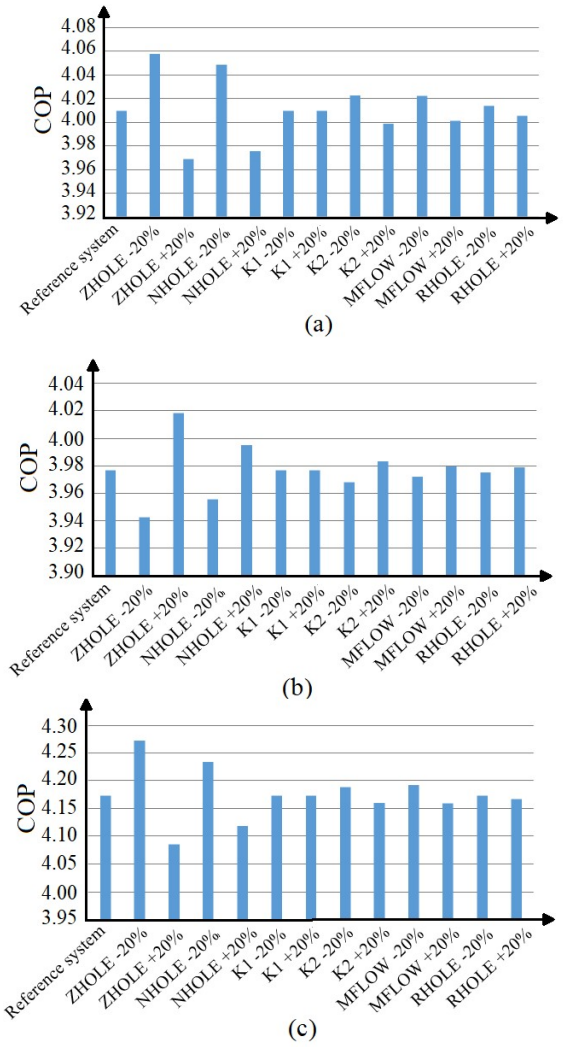

Figure 8. COP values for various parameters in sensitivity analysis for (a) Oslo, (b) Stavanger, and (c) Tromsø climatic conditions.

As Figure 9 shows, in Oslo and Tromsø climate, a decrease in the borehole length yielded a decrease in both the extracted energy from the borehole and the compressor energy use (top picture in Figure 9). However, the ratio of extracted energy from the borehole to the compressor energy use increased as the borehole length decreased, 1.33% and 11.97% for Oslo and Tromsø, respectively. Therefore, the COP increased (cases (c) and (a) in Figure 8). A different trend happened for Stavanger climate; a decrease in the length of borehole led the extracted energy from the borehole to decrease and the compressor energy use to increase resulting in a decrease in the COP value. It should be also noted that the GSHP could cover almost the whole heating needs in the Stavanger climate so that a trivial amount of energy need for heating was supplied by the peak load heating.

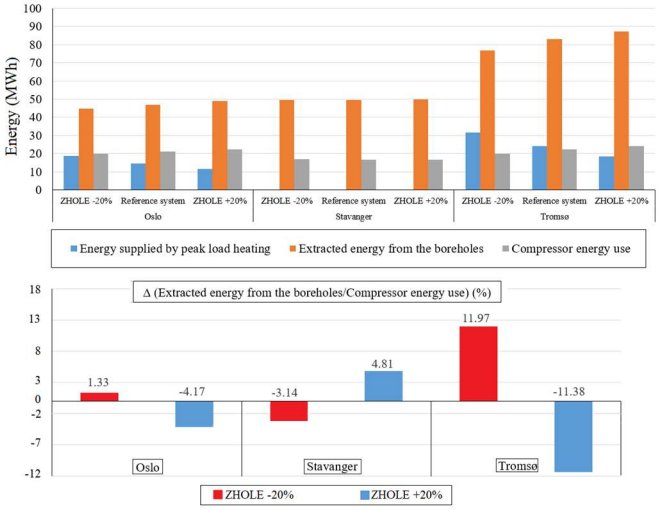

Figure 9. Amount of energy supplied, extracted, and used by different part of GSHP system (top) and ratio variation of borehole extraction energy to compressor energy use (bottom)

Table 5 shows the optimized input parameters, introduced in Table 4, which resulted in minimum delivered energy to the building.

Table 5. Optimized input parameters and the corresponding minimum delivered energy values at three different locations

Parameter	Oslo	Stavanger	Tromsø
Borehole depth (m)	400	400	400
Number of boreholes	20	20	20
Mas flow rate (kg/s)	5	3	5
Tank radius (m)	1	0.2	1
Window U-value (W/(m^2.K))	0.6	0.7	0.6
Delivered energy of the Reference system (kWh/year)	20 741	17 153	27 193
Delivered energy of the optimal system (kWh/year)	16 127	16 290	23 939

The maximum values of the mass flow rate, length and the number of boreholes, and the tank radius were chosen in the optimization process for the Oslo and Tromsø cases. Nevertheless, the same values did not result in the minimum delivered energy for the Stavanger case. The largest decrease was for the Oslo case, where the annual delivered energy was reduced by 4 614 kWh. In the

Stavanger case, there was a little change, 863 kWh, while for the Tromsø case it reduced by 3 254 kWh. These values correspond to approximately 22%, 5%, and 12% reduction of the delivered energy compared to the reference system in Oslo, Stavanger, and Tromsø cases respectively.

Conclusion

This paper dealt with sensitive analysis and optimization of the GSHP system. The simulations were performed using the building simulation software IDA-ICE and the generic optimization tool GenOpt. In the first step, the ground source borehole model was validated by available measured data and the simulation results were in good agreement with the measured data. The sensitive analysis showed that the borehole depth was the most effective and decreasing the borehole depth by 20% led the energy supplied by the peak load heating to increase up to 28%, 108%, and 31% for Oslo, Stavanger, and Tromsø climatic conditions, respectively. Furthermore, the optimization process revealed that the annual delivered energy to the building was decreased by approximately 22%, 5%, and 12% compared to the reference system in Oslo, Stavanger, and Tromsø cases respectively. Future work on the optimization and sensitive analysis could include a life cycle cost and a life cycle CO_2 emission for different alternatives along with delivered energy simultaneously. It can provide readers with more practical insights about the effective parameters on the system performance.

References

Ally, M.R., Munk, J.D., Baxter, V.D. and Gehl, A.C. (2015). Exergy analysis of a two-stage ground source heat pump with a vertical bore for residential space conditioning under simulated occupancy. *Applied Energy 155*, 502–514.

American Society of Heating, Ventilating, and Air Conditioning Engineers (ASHRAE). Guideline 14-(2014), Measurement of Energy and Demand Savings; Technical Report; American Society of Heating, Ventilating, and Air Conditioning Engineers: Atlanta, GA, USA.

Building Technical Regulations with guidance (2017). (*TEK 17*) (in Norwegian).

Chen, Y., Wang, J., Ma, C. and Shi, G. (2019). Multicriteria performance investigations of a hybrid ground source heat pump system integrated with concentrated photovoltaic thermal solar collectors, *Energy Conversion and Management 197*, 111862.

Directorate of the Labor Inspectorate, Climate and air quality in the workplace (2016) (in Norwegian). Accessible:https://www.arbeidstilsynet.no/contentassets/3f86f6d2038348d18540404144f76a22/luftkvalitet-pa-arbeidsplassen.pdf

Emmi, G., Zarrella, A., De Carli, M. and Galgaro, A. (2015). An analysis of solar assisted ground source heat pumps in cold climates, *Energy Conversion and Management 106*, 660–675.

Fadejev, J. and Kurnitski, J. (2015). Geothermal energy piles and boreholes design with heat pump in a whole building simulation software, *Energy and buildings 106*, 23–34.

Madessa, H.B., Torger, B., Bye, P.F. and Erlend, A. (2017). Parametric Study of a Vertically Configured Ground Source Heat Pump System. *Energy Procedia 111*, 1040–1049.

Metz, B., Davidson, Davidson, O., Bosch, P., Dave, R. and Meyer, L. (2007). *Mitigation of climate change*, Cambridge University Press, Cambridge (UK).

Naranjo-Mendoza, C., Oyinlola, M.A., Wright, A.J. and Greenough, R.M. (2019). Experimental study of a domestic solar-assisted ground source heat pump with seasonal underground thermal energy storage through shallow boreholes, *Applied Thermal Engineering 162*, 114218.

Nord, N., Qvistgaard, L.H. and Cao, G. (2016). Identifying key design parameters of the integrated energy system for a residential Zero Emission Building in Norway. *Renewable Energy 87,* 1076–1087.

Nord, N. (2017). Building Energy Efficiency in Cold Climates, *Encyclopedia of Sustainable Technologies*, 149–157.

Norwegian Standard (2012). *Criteria for passive houses and low energy buildings*, *Non-residential buildings*, *(NS-3701)* (in Norwegian).

Norwegian Standard (2014). *Calculation of energy performance of buildings - Method and data*, (*NS 3031*) (in Norwegian).

Norwegian book prices (Norsk Prisbok) (2019). *Norconsult Informasjonssystemer AS*, https://www.norskprisbok.no/WhatIsNP.aspx

Wang, G., Wang, W., Luo, J. and Zhang, Y. (2019). Assessment of three types of shallow geothermal resources and ground-source heat-pump applications in provincial capitals in the Yangtze River Basin, China, *Renewable and Sustainable Energy Reviews 111*, 392–421.

Zhang, P., Wang, B., Wu, W., Shi, W. and Li, X. (2015). Heat recovery from Internet data centers for space heating based on an integrated air conditioner with thermosyphon, *Renewable Energy 80* 396–406.